N92-19742

A TWO-DIMENSIONAL TIME DOMAIN NEAR ZONE TO FAR ZONE TRANSFORMATION

by

Raymond Luebbers, Deirdre Ryan, John Beggs
and Karl Kunz

Electrical and Computer Engineering Department
The Pennsylvania State University
University Park, PA 16802

May 1991

Abstract

In a previous paper [1] a time domain transformation useful for extrapolating three dimensional near zone finite difference time domain (FDTD) results to the far zone was presented. In this paper the corresponding two dimensional transform is outlined. While the three dimensional transformation produced a physically observable far zone time domain field, this is not convenient to do directly in two dimensions, since a convolution would be required. However, a representative two dimensional far zone time domain result can be obtained directly. This result can then be transformed to the frequency domain using a Fast Fourier Transform, corrected with a simple multiplicative factor, and used, for example, to calculate the complex wideband scattering width of a target. If an actual time domain far zone result is required it can be obtained by inverse Fourier transform of the final frequency domain result.

Introduction

A previous paper [1] described a method for transforming near zone Finite Difference Time Domain (FDTD) results directly to the far zone without first transforming to the frequency domain. This far zone field could then be used to compute the scattering cross section of an illuminated target or an antenna radiation pattern over the entire frequency band of the FDTD calculations. A similar result was published in [2]. In this paper the corresponding two dimensional transform is presented, and validated by comparison with calculated results for a perfectly conducting circular cylinder.

Approach

In [1] the frequency domain far zone transformation equations were Fourier transformed to the time domain and used in that form to derive an approach to transform near zone FDTD fields to the far zone directly in the time domain. Our approach here will be to present the fundamental frequency domain equations for both two and three dimensions, and by comparing them obtain the factor needed to convert the three dimensional far zone transform to function in two dimensions.

We again surround the scatterer with a closed surface S', and consider that equivalent tangential electric and magnetic time harmonic surface currents may exist on this surface. Referring to [3], we obtain the vector potentials for the three dimensional case as

$$\bar{A} = \frac{e^{-jkr}}{4\pi r} \int_{S'} \bar{J}_s \, e^{jk\bar{r}'\cdot\hat{r}} \, ds' \qquad (1)$$

$$\bar{F} = \frac{e^{-jkr}}{4\pi r} \int_{S'} \bar{M}_s \, e^{jk\bar{r}'\cdot\hat{r}} \, ds' \qquad (2)$$

with $j=\sqrt{-1}$, $k = \omega\sqrt{\mu\epsilon}$ (the wave number), $\hat{r}$ the unit vector to the far zone field point, $\bar{r}'$ the vector to the source point of integration, r the distance to the far zone field point, and S' the closed surface surrounding the scatterer.

The far zone frequency domain electric fields of the scatterer are then obtained from

$$E_\theta = -j\omega\mu A_\theta - j\omega\sqrt{\mu\epsilon}\, F_\phi \qquad (3)$$

$$E_\phi = -j\omega\mu A_\phi + j\omega\sqrt{\mu\epsilon}\, F_\theta \qquad (4)$$

One can then easily convert to radar cross section (RCS), if desired, by applying

$$\sigma_{3D} = \lim_{r\to\infty} \left(4\pi r^2 \frac{|E^s_{3D}|^2}{|E^i|^2}\right) \qquad (5)$$

where E^s_{3D} is either E_θ or E_ϕ of (2) or (3), and E^i is the incident plane wave electric field.

In [1] the equations corresponding to (1,2) were easily transformed to the time domain since the exponential phase term inside the integrals corresponds to a time shift relative to an arbitrary time reference point. Equations corresponding to (2,3) were also readily transformed to the time domain since the $j\omega$ factor in these equations corresponds to a time derivative. Thus the resulting time domain fields can be obtained conveniently directly in the time domain, as shown in [1].

Now consider the corresponding equations in two dimensions. The vector potentials are given by

$$\bar{A} = \frac{e^{-jk\rho}}{\sqrt{8jk\pi\rho}} \int_{S'} \bar{J}_s \, e^{jk\rho'\cos(\phi-\phi')} \, ds' \tag{6}$$

$$\bar{F} = \frac{e^{-jk\rho}}{\sqrt{8jk\pi\rho}} \int_{S'} \bar{M}_s \, e^{jk\rho'\cos(\phi-\phi')} \, ds' \tag{7}$$

where ρ' and ϕ' are the coordinates of the source point of integration, and ρ and ϕ the coordinates of the far zone field point. The corresponding far zone radiated fields are obtained from

$$E_z = -j\omega\mu A_z + j\omega\sqrt{\mu\epsilon}\, F_\phi \tag{8}$$

$$E_\phi = -j\omega\mu A_\phi - j\omega\sqrt{\mu\epsilon}\, F_z \tag{9}$$

Also, the two dimensional scattering width is defined as

$$\sigma_{2D} = \lim_{\rho\to\infty} \left(2\pi\rho \frac{|E^s_{2D}|^2}{|E^i|^2}\right) \tag{10}$$

where E^s_{2D} is either E_z or E_ϕ of (8,9).

The approach applied in [1] cannot be conveniently applied in the two dimensional case due to the factor of $1/\sqrt{jk}$ (actually $1/\sqrt{j\omega\sqrt{\mu\epsilon}}$) in (6,7). In order to evaluate the Fourier transform of (6,7) directly in the time domain a convolution operation would be required. To avoid this complication our approach will be to modify the results in [1] to provide representative two dimensional time domain far zone fields which can then be converted to the actual frequency domain fields by a multiplication in the frequency domain rather than the time domain convolution. Should the actual time domain far zone fields be required, they can then be obtained by an additional Fourier transform of these results back to the time domain.

In order to convert our previous three dimensional results to two dimensions, we compare the two sets of equations. First, comparing (3,4) with (8,9), since the spherical unit θ vector is equal to the negative of the cylindrical unit z vector, (3,4) and (8,9) correspond exactly, and no adjustment between two and three dimensional transforms is needed.

Next, comparing (1,2) with (6,7) the r^2 and ρ factors are compensated by the definitions in (5) and (10) respectively, as expected, and no compensation is needed here either.

Finally, consider equations (1,2) vs (6,7). The additional dimension of integration in (1,2) is compensated for by defining a scattering width per unit length (in z) in (10). This

corresponds in (1,2) to having no z variation and integrating the z' variable over a unit distance. The exponents provide equivalent phase (time) delays and need not be compensated for. Considering the remaining factors, it is easily determined that in the frequency domain, the relationship between far zone electric fields obtained from a three dimensional far zone transformation with no z variation and the two dimensional far zone fields is

$$E^s_{2D} = \sqrt{\frac{2\pi c}{j\omega}}\; E^s_{3D} \tag{11}$$

where $c = 1/\sqrt{\mu\epsilon}$.

With these results the time domain far zone transform given in [1] can be easily adapted to two dimensions as follows:

1) Consider only the field components and corresponding surface currents excited in the two dimensional problem. For example, for a TE_z computation only H_z, E_x, E_y, and the corresponding surface currents are included.

2) Calculate the far zone time domain fields using the method described in [1], but for a two dimensional integration surface which encloses the scatterer. Let δz, the z coordinate unit cell dimension used in [1], equal 1 (meter). (This field is not a physically observable field. It represents the radiation from a unit length of the scatterer in the time domain.)

3) Fourier transform the result of step 2) and multiply the result by the factor in (11). This result is the frequency domain two dimensional far zone field, which can then be used in

(10) to calculate the scattering width as a function of frequency.

4) If the actual time domain two dimensional far zone field is desired, it can be obtained by an additional Fourier transformation of the result obtained in 3) back to the time domain.

Demonstration

In order to demonstrate the capabilities of the above approach a pair (TE_z and TM_z) of FDTD codes were developed from the three dimensional FDTD code described in [1]. These codes utilize second order Mur absorbing boundary conditions acting on the electric fields. The test geometry was a circular perfectly conducting cylinder of radius 0.25 meters.

Both TE and TM polarization was considered, and two sets of calculations were made for each polarization. For the first set the FDTD cells were 1 cm squares, with a problem space 200x200 cells. For the second set the cells were 0.5 cm squares in a 500x500 cell problem space. On a 25 MHz 486 PC (approximately 1 MFLOP) each of the first set required about 20 minutes to compute, with each of the second set requiring a few minutes less than 2 hours.

For all cases the incident plane wave traveled in the x direction, backscatter was calculated, and 2048 time steps were evaluated. In order to clearly show the response, not all time steps are included in the Figures.

Figure 1 shows the relative far zone fields computed directly in the time domain as outlined above for the TM polarization. The small ripple at approximately 15 ns on Figure 1 is due to reflections from the Mur outer boundary. Figures 2 and 3 show comparison with the exact solution for the scattering

width amplitude and phase. The upper frequency limit of 3.0 GHz corresponds to 10 cells per wavelength. The agreement is quite good.

A similar set of data for TE polarization is shown in Figures 4-6. The time domain far zone results in Figure 4 has ripples in the 6-8 ns range due to the staircasing of the round cylinder with square FDTD cells. The small negative pulse at 10 ns is the creeping wave which has traveled around the cylinder. Again, there is a small ripple at 14 ns due to the Mur boundary reflection. This is the difficult polarization for approximating a smooth surface with a "staircased" FDTD code, yet the agreement in Figures 5 and 6 is reasonably good, reproducing the first 6 1/2 ripples in the scattering width.

The above calculations are repeated in Figures 7-13 with a greater expenditure of computer resources. For these results the cell size of 0.5 cm changes the 3.0 GHz upper frequency limit of the plots to correspond to 20 cells per wavelength. The improvement in the agreement with the exact solution is clear, indicating the accuracy that can be obtained from this approach. Note especially Figure 12, which shows on a expanded dB scale agreement with the exact solution within a fraction of a dB for the first 9 lobes of the response.

Conclusions

A simple approach to calculating a wide bandwidth time domain transformation of near zone FDTD fields to the far zone has been presented. It is based on simple modifications to the previous three dimensional method presented in [1]. Results obtained using this transformation show good agreement with the exact solution for a circular cylinder for both polarizations.

References

1. R. J. Luebbers, K. S. Kunz, M. Schneider, and F. Hunsberger, "A Finite Difference Time-Domain Near Zone to Far Zone Transformation," IEEE Trans. Ant. Prop., Vol. 39, No. 4, April 1991, pp 429-433.

2. K. S. Yee, D. Ingham, and K. Shlager, "Time-Domain Extrapolation to the Far Field Based on FDTD Calculations," IEEE Trans. Ant. Prop., Vol. 39, No. 3, March 1991, pp 410-412.

3. R. F. Harrington, Time-Harmonic Electromagnetic Fields, McGraw-Hill, 1961.

Figure Titles

Fig 1. Far Zone relative electric field vs time for TM_z polarized incident Gaussian pulsed plane wave illuminating a perfectly conducting circular cylinder. FDTD cells are 1 cm squares.

Fig 2. Scattering width amplitude obtained from far zone time domain results and compared with exact solution. FDTD cells are 1 cm squares.

Fig 3. Scattering width phase obtained from far zone time domain results and compared with exact solution. FDTD cells are 1 cm squares.

Fig 4. Far Zone relative electric field vs time for TE_z polarized incident Gaussian pulsed plane wave illuminating a perfectly conducting circular cylinder. FDTD cells are 1 cm squares.

Fig 5. Scattering width amplitude obtained from far zone time domain results and compared with exact solution. FDTD cells are 1 cm squares.

Fig 6. Scattering width phase obtained from far zone time domain results and compared with exact solution. FDTD cells are 1 cm squares.

Fig 7. Far Zone relative electric field vs time for TM_z polarized incident Gaussian pulsed plane wave illuminating a perfectly conducting circular cylinder. FDTD cells are 0.5 cm squares.

Fig 8. Scattering width amplitude obtained from far zone time domain results and compared with exact solution. FDTD cells are 0.5 cm squares.

Fig 9. Scattering width phase obtained from far zone time domain results and compared with exact solution. FDTD cells are 0.5 cm squares.

Fig 10. Far Zone relative electric field vs time for TE_z polarized incident Gaussian pulsed plane wave illuminating a perfectly conducting circular cylinder. FDTD cells are 0.5 cm squares.

Fig 11. Scattering width amplitude obtained from far zone time domain results and compared with exact solution. FDTD cells are 0.5 cm squares.

Fig 12. Scattering width amplitude obtained from far zone time domain results and compared with exact solution on an expanded dB scale. FDTD cells are 0.5 cm squares.

Fig 13. Scattering width phase obtained from far zone time domain results and compared with exact solution. FDTD cells are 0.5 cm squares.

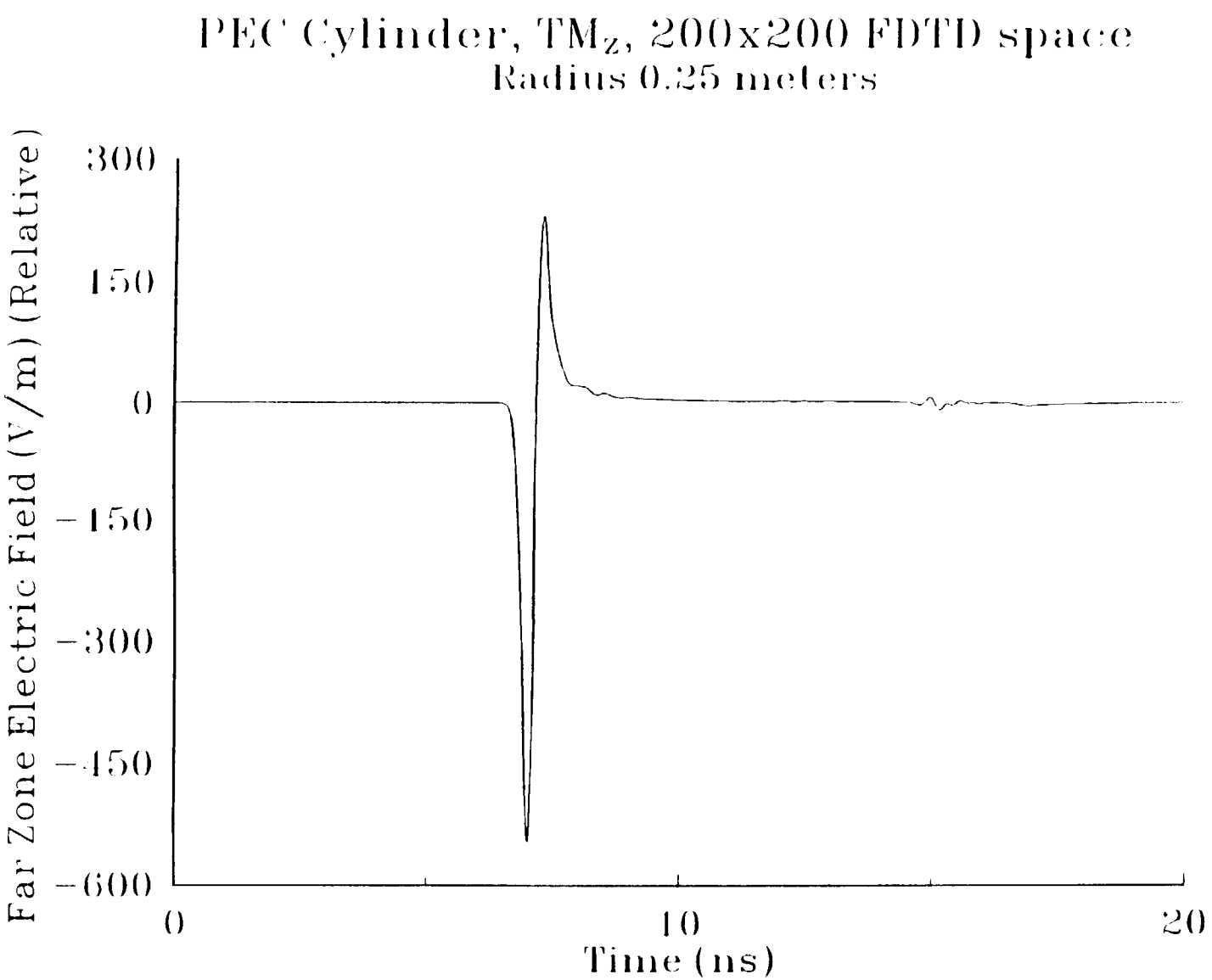
PEC Cylinder, TMz, 200x200 FDTD space
Radius 0.25 meters
Far Zone Electric Field (V/m) (Relative)
300
150
0
−150
−300
−450
−600
0
10
20
Time (ns)

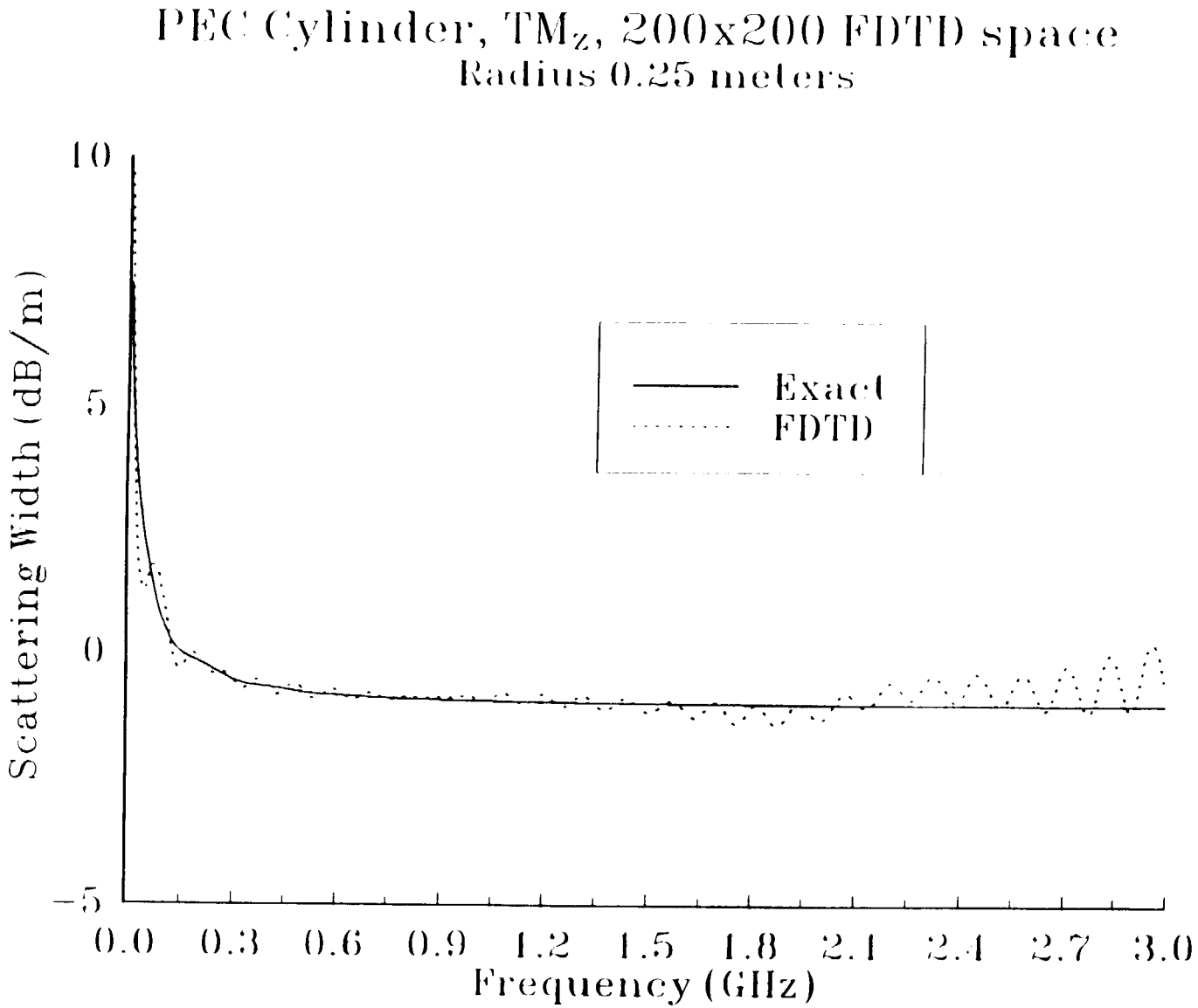
PEC Cylinder, TMz, 200x200 FDTD space
Radius 0.25 meters
Scattering Width (dB/m)
10
5
0
−5
Exact
FDTD
0.0
0.3
0.6
0.9
1.2
1.5
1.8
2.1
2.4
2.7
3.0
Frequency (GHz)

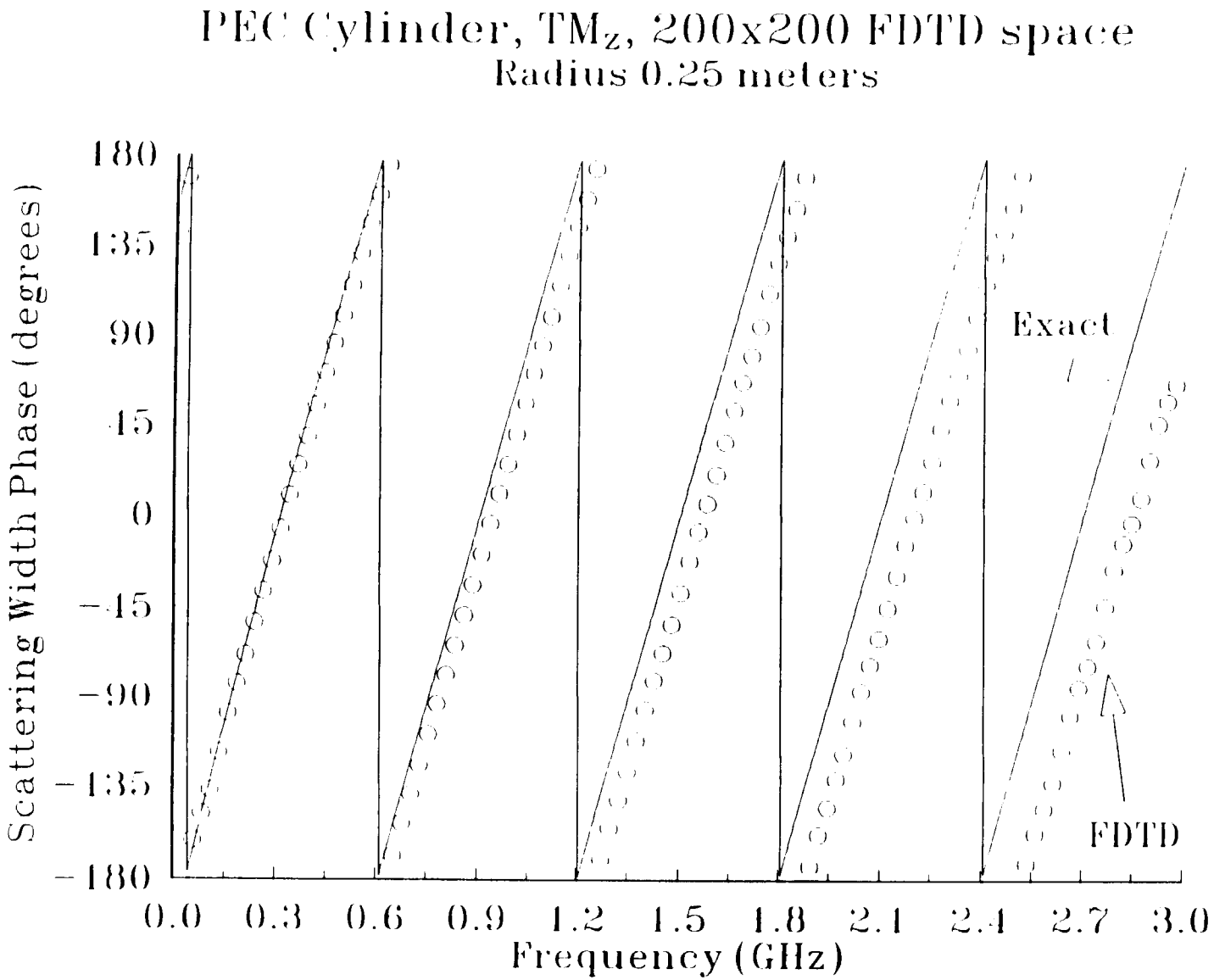
PEC Cylinder, TMz, 200x200 FDTD space
Radius 0.25 meters
Scattering Width Phase (degrees)
180
135
90
45
0
-45
-90
-135
-180
0.0
0.3
0.6
0.9
1.2
1.5
1.8
2.1
2.4
2.7
3.0
Frequency (GHz)
Exact
FDTD

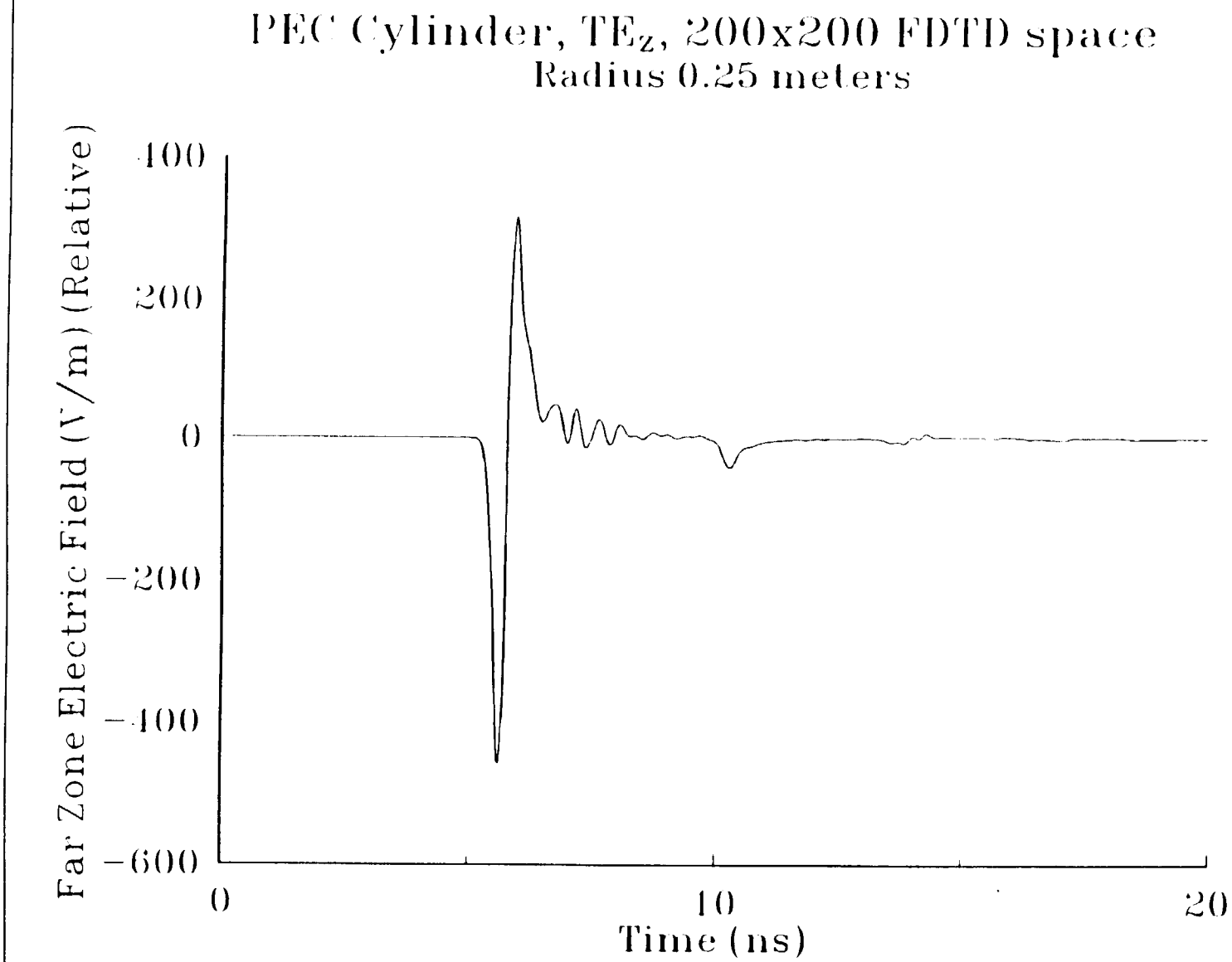
PEC Cylinder, TEz, 200x200 FDTD space
Radius 0.25 meters
Far Zone Electric Field (V/m) (Relative)
400
200
0
−200
−400
−600
0
10
20
Time (ns)

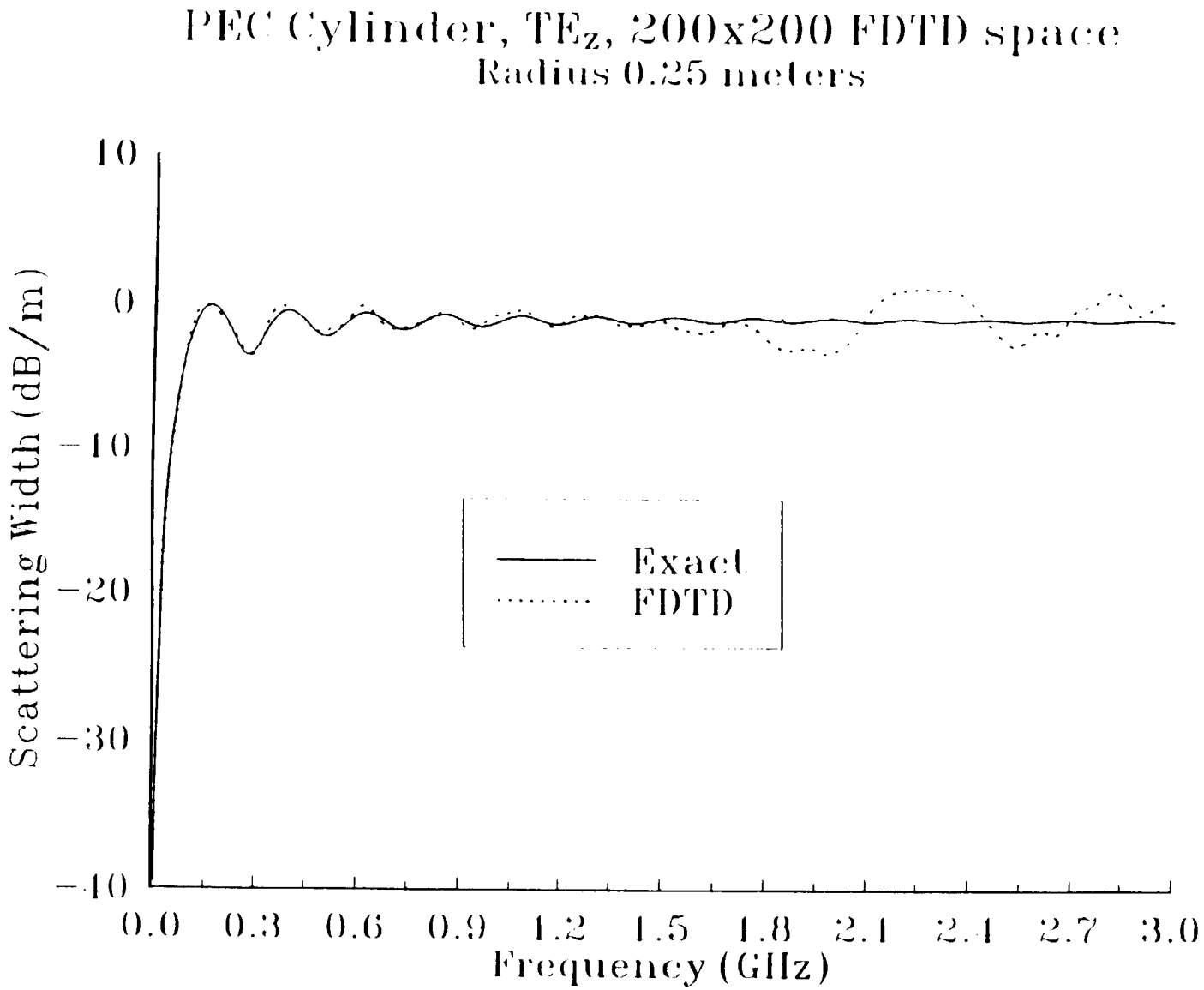
PEC Cylinder, TEz, 200x200 FDTD space
Radius 0.25 meters
Scattering Width (dB/m)
10
0
−10
−20
−30
−40
0.0
0.3
0.6
0.9
1.2
1.5
1.8
2.1
2.4
2.7
3.0
Frequency (GHz)
Exact
FDTD

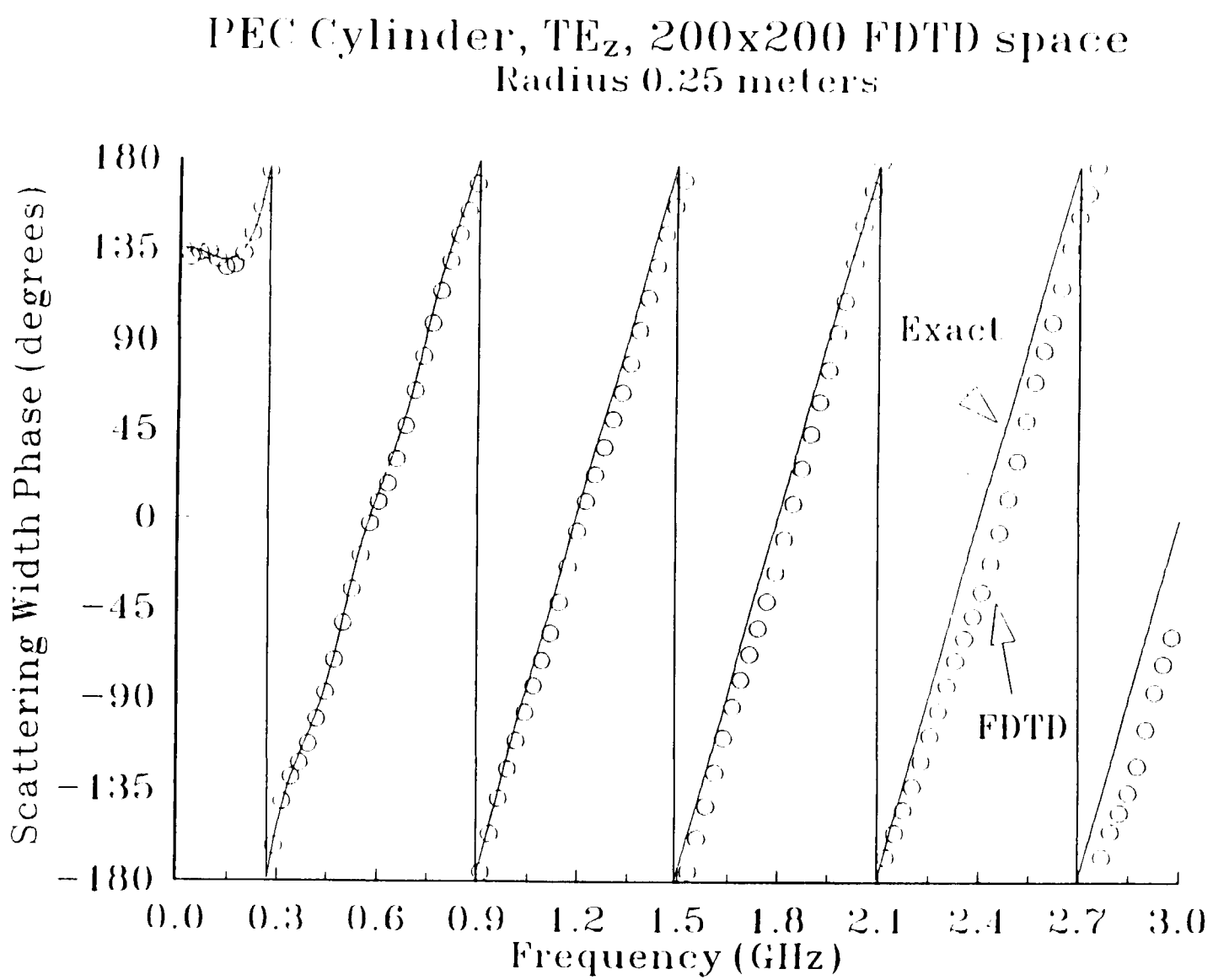
PEC Cylinder, TEz, 200x200 FDTD space
Radius 0.25 meters
Scattering Width Phase (degrees)
180
135
90
45
0
-45
-90
-135
-180
0.0
0.3
0.6
0.9
1.2
1.5
1.8
2.1
2.4
2.7
3.0
Frequency (GHz)
Exact
FDTD

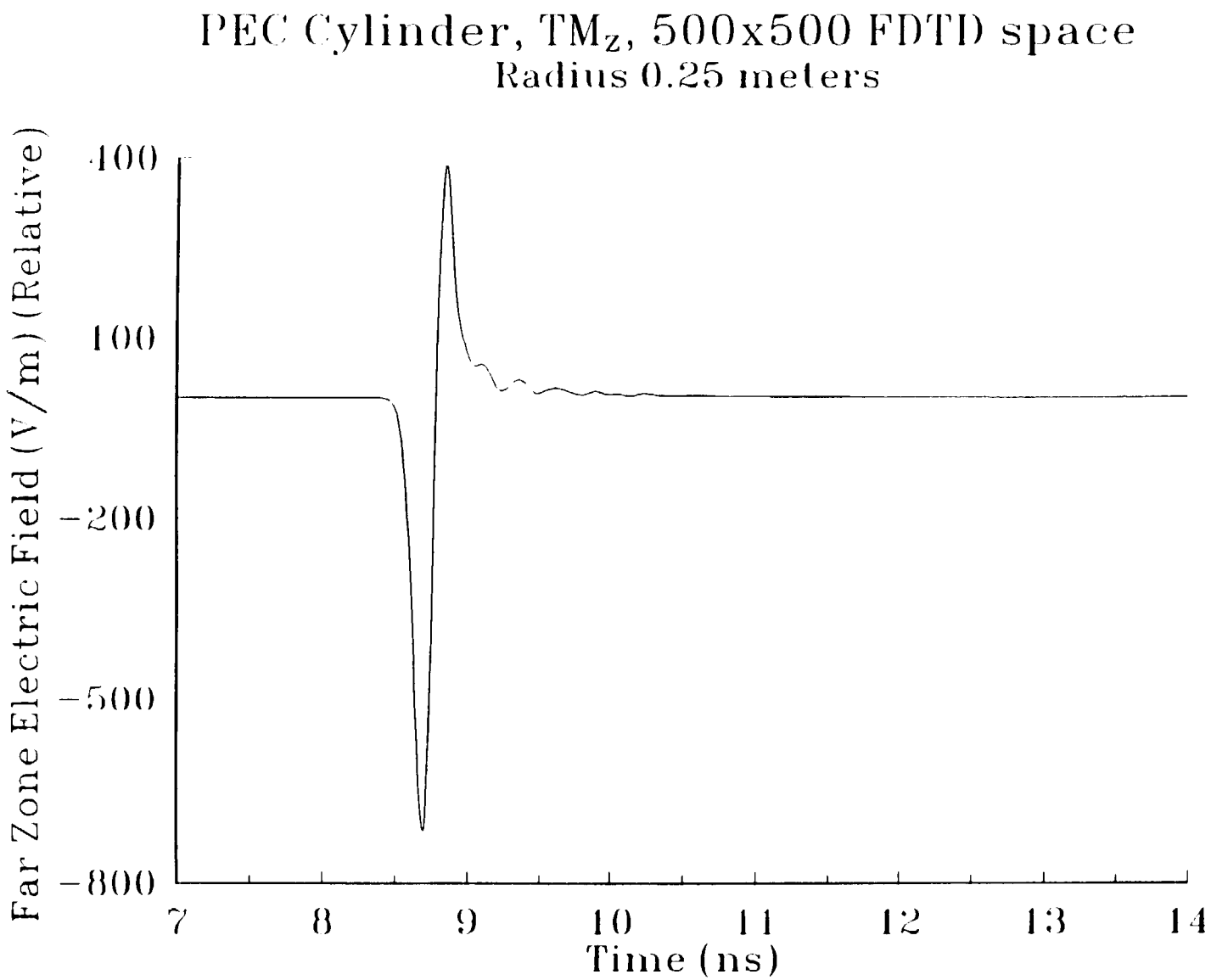
PEC Cylinder, TMz, 500x500 FDTD space
Radius 0.25 meters
Far Zone Electric Field (V/m) (Relative)
400
100
-200
-500
-800
7
8
9
10
11
12
13
14
Time (ns)

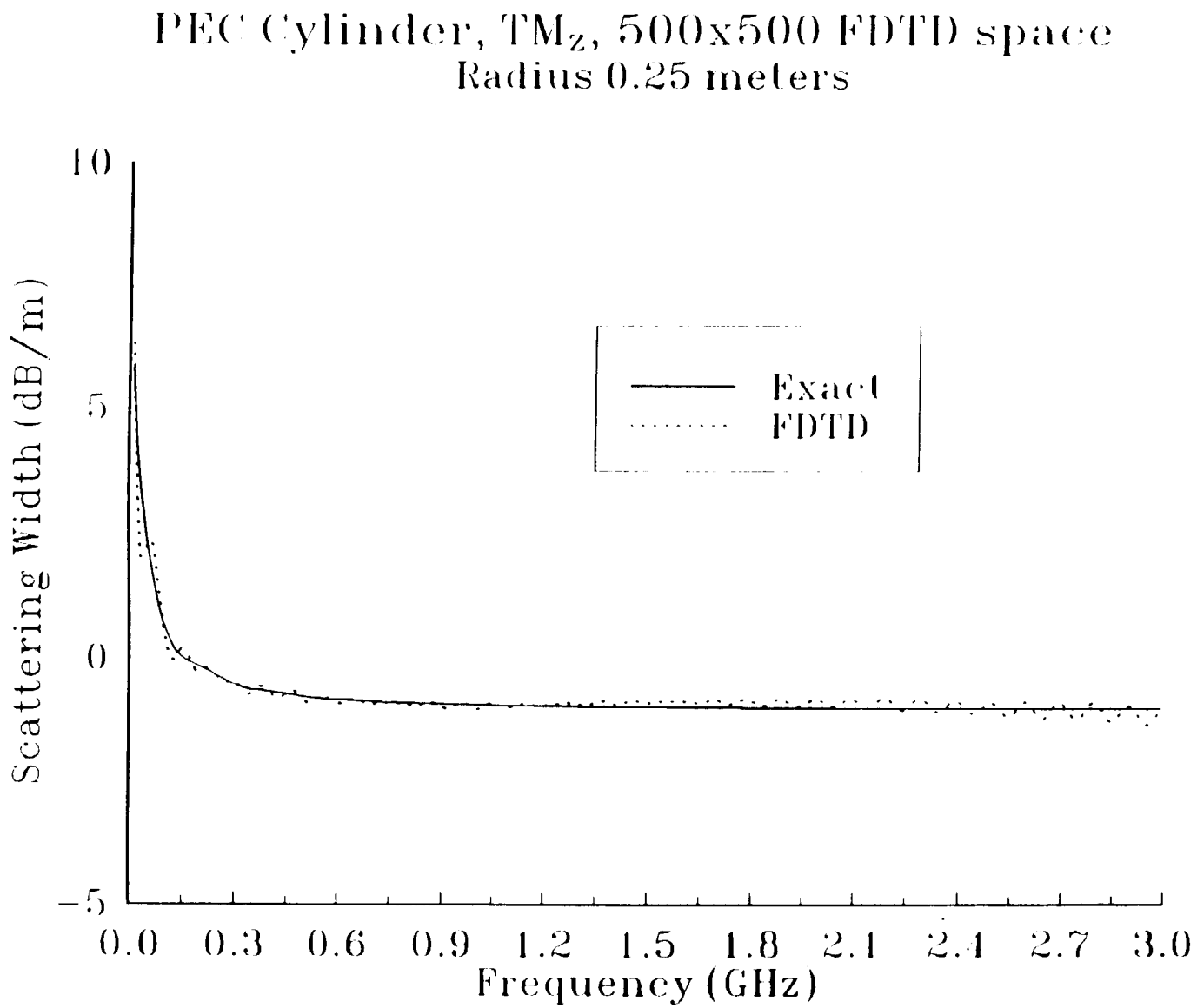
PEC Cylinder, TMz, 500x500 FDTD space
Radius 0.25 meters
Scattering Width (dB/m)
10
5
0
−5
Exact
FDTD
0.0
0.3
0.6
0.9
1.2
1.5
1.8
2.1
2.4
2.7
3.0
Frequency (GHz)

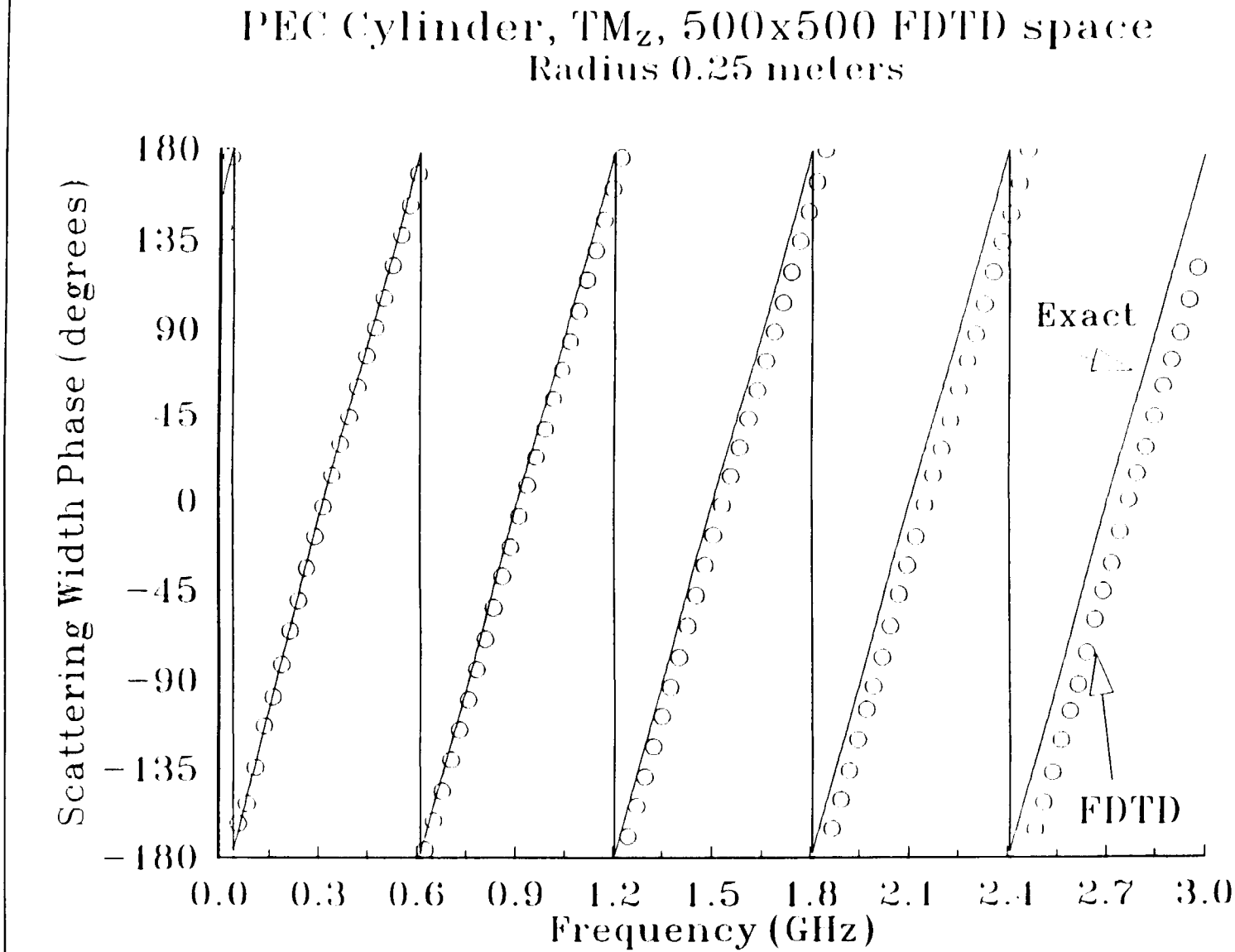
PEC Cylinder, TMz, 500x500 FDTD space
Radius 0.25 meters
Scattering Width Phase (degrees)
180
135
90
45
0
−45
−90
−135
−180
0.0
0.3
0.6
0.9
1.2
1.5
1.8
2.1
2.4
2.7
3.0
Frequency (GHz)
Exact
FDTD

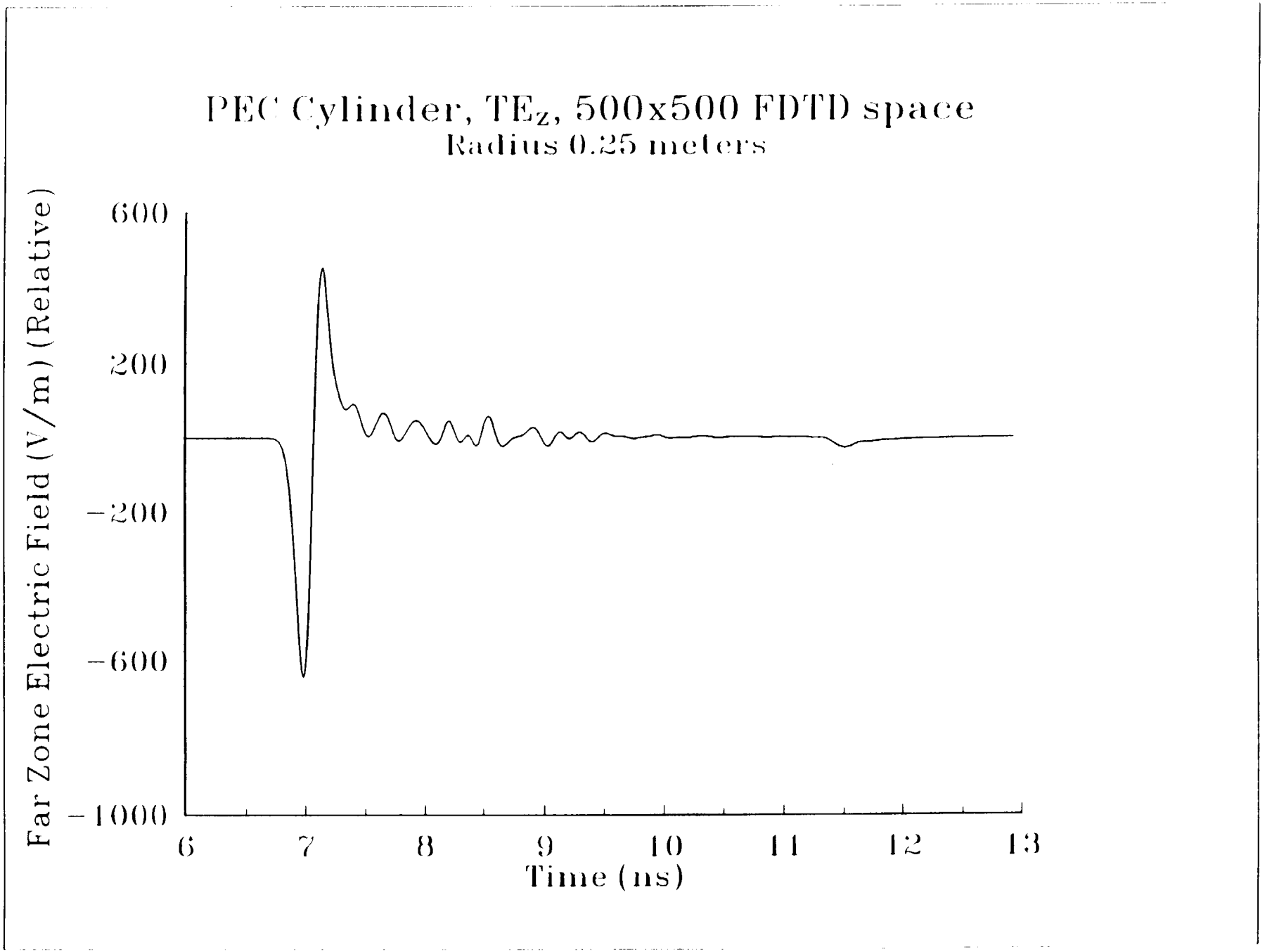
PEC Cylinder, TEz, 500x500 FDTD space
Radius 0.25 meters
Far Zone Electric Field (V/m) (Relative)
600
200
-200
-600
-1000
6
7
8
9
10
11
12
13
Time (ns)

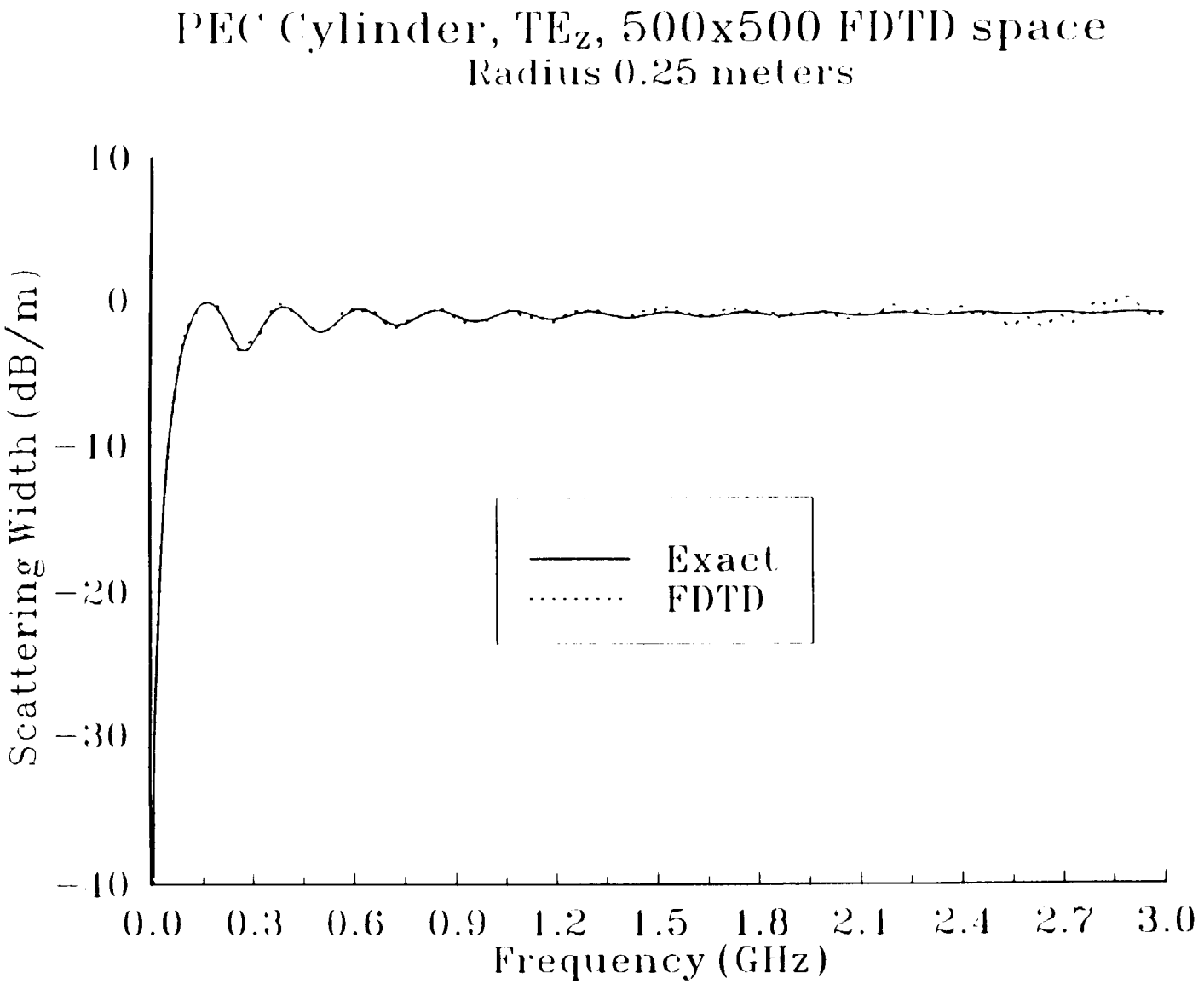
PEC Cylinder, TEz, 500x500 FDTD space
Radius 0.25 meters
Scattering Width (dB/m)
10
0
−10
−20
−30
−40
0.0
0.3
0.6
0.9
1.2
1.5
1.8
2.1
2.4
2.7
3.0
Frequency (GHz)
Exact
FDTD

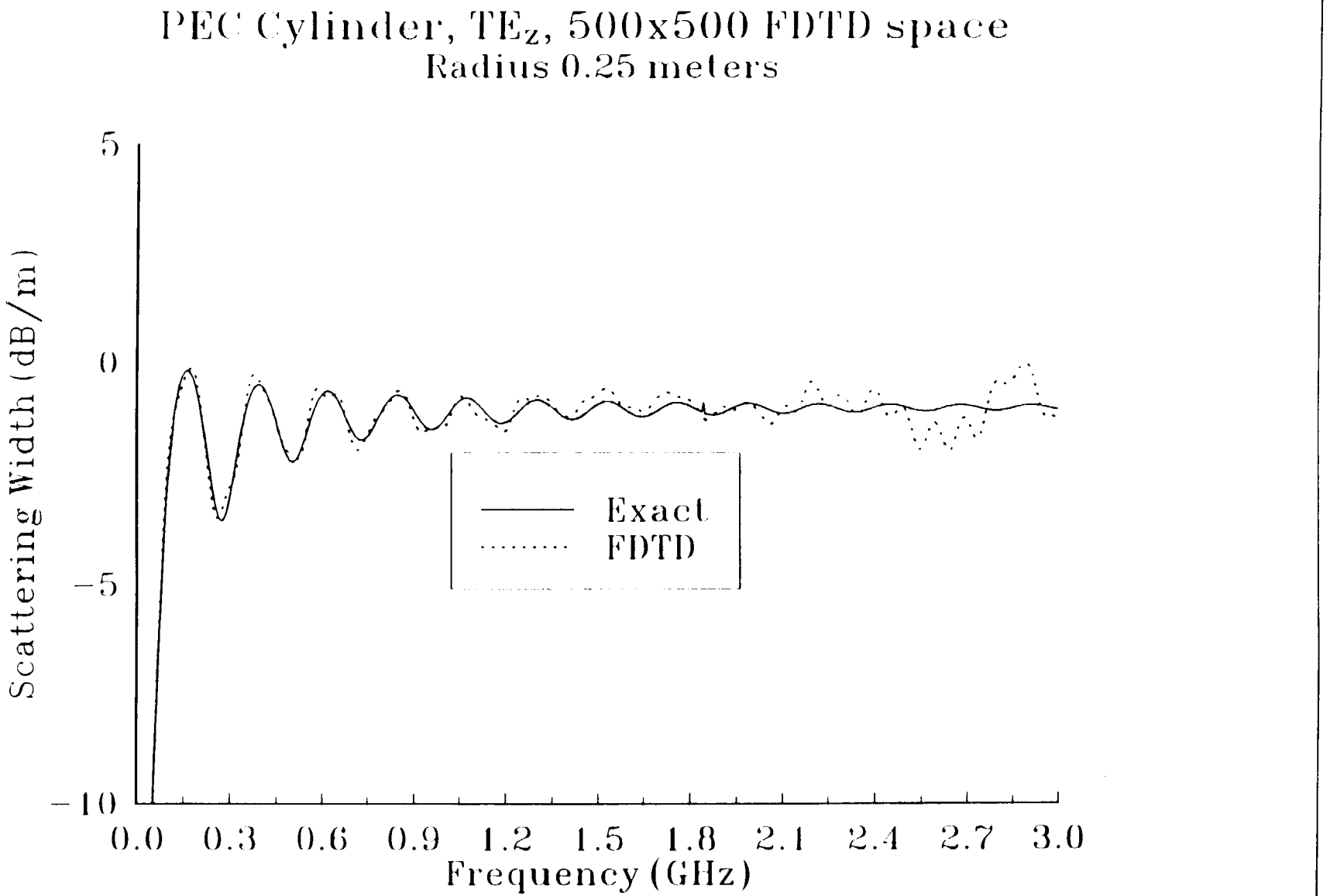
PEC Cylinder, TEz, 500x500 FDTD space
Radius 0.25 meters
Scattering Width (dB/m)
5
0
−5
−10
0.0
0.3
0.6
0.9
1.2
1.5
1.8
2.1
2.4
2.7
3.0
Frequency (GHz)
Exact
FDTD

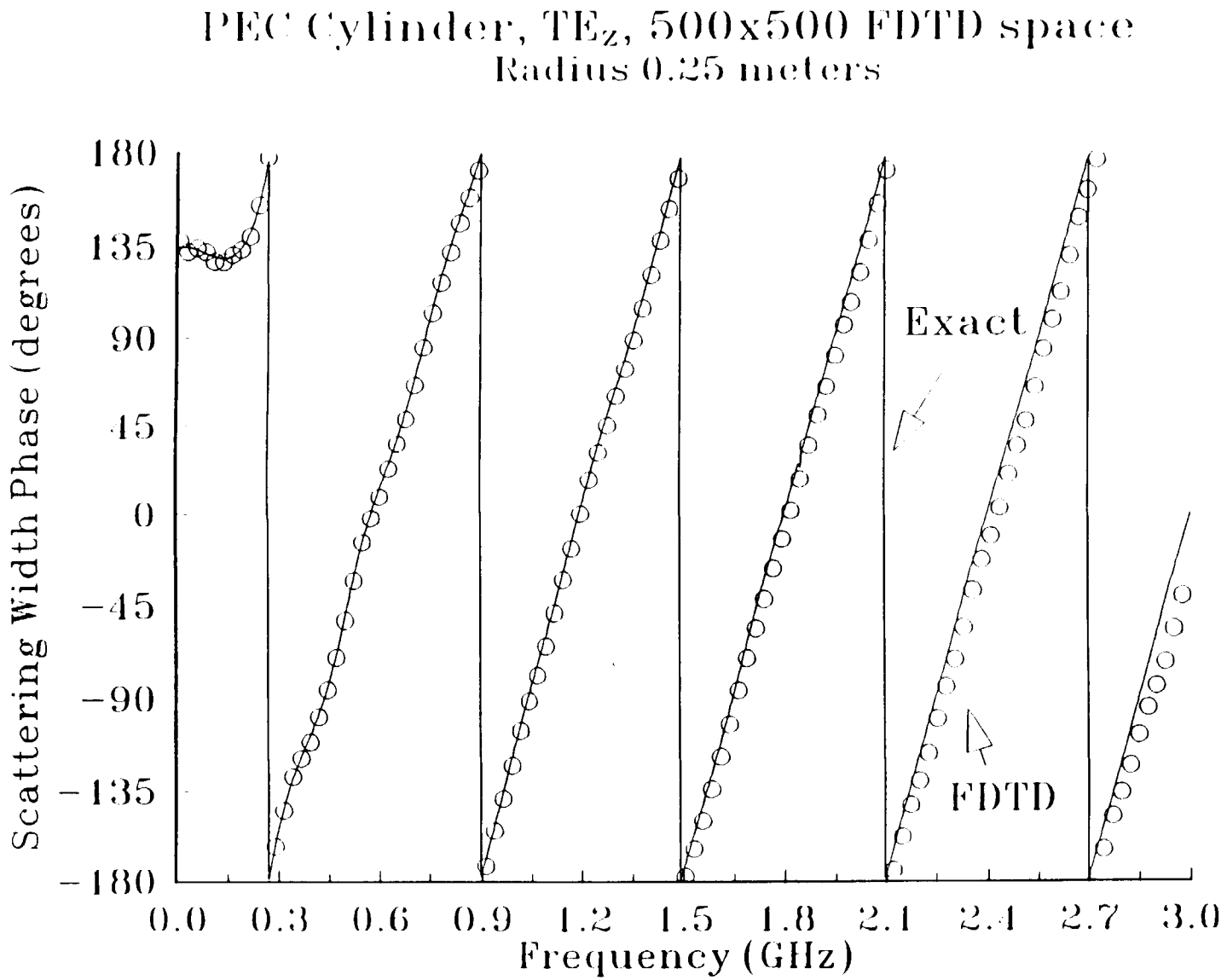
PEC Cylinder, TEz, 500x500 FDTD space
Radius 0.25 meters
Scattering Width Phase (degrees)
180
135
90
45
0
−45
−90
−135
−180
0.0
0.3
0.6
0.9
1.2
1.5
1.8
2.1
2.4
2.7
3.0
Frequency (GHz)
Exact
FDTD